



Applications of neural networks for the novel designed of nonlinear fractional seventh order singular system

Zulqurnain Sabir¹, Muhammad Asif Zahoor Raja², Tri Gia Nguyen³, Irwan Fathurochman^{4,a}, R. Sadat⁵, and Mohamed R. Ali^{6,7,b} 

¹ Department of Mathematics and Statistics, Hazara University, Mansehra, Pakistan

² Future Technology Research Center, National Yunlin University of Science and Technology, 123 University Road, Section 3, Douliou, Yunlin 64002, Taiwan, ROC

³ FPT University, Da Nang 50509, Vietnam

⁴ Department of Islamic Educational Management, Institute Agama Islam Negeri Curup, Rejang Lebong, Indonesia

⁵ Department of Basic Science, Faculty of Engineering at Zagazig, Zagazig University, Zagazig, Egypt

⁶ Faculty of Engineering and Technology, Future University, Cairo, Egypt

⁷ Department of Basic Science, Faculty of Engineering at Benha, Benha University, Benha 13512, Egypt

Received 30 July 2021 / Accepted 13 January 2022

© The Author(s), under exclusive licence to EDP Sciences, Springer-Verlag GmbH Germany, part of Springer Nature 2022

Abstract The purpose of this work is to design a novel nonlinear fractional seventh kind of singular (NSKS) Emden–Fowler model (EFM), i.e., NSKS-EFM together with its six categories. The novel design of NSKS-EFM is obtained with the use of typical EFM of the second kind. The shape factor and singular points detail is accessible for all six categories of the NSKS-EFM. The singular problems arise in the mathematical engineering problems, like as inverse models, creep or viscoelasticity problems. To check the correctness of the designed novel NSKS-EFM, three different cases of the first category will be solved by using the supervised neural networks (SNNs) together with the Levenberg–Marquardt backpropagation method (LMBM), i.e., SNNs-LMBM. A reference dataset based on the exact solutions with the SNNs-LMBM will be performed for each case of the novel NSKS-EFM. The obtained approximate solutions of all three cases of the first group based on the novel NSKS-EFM is available using the testing, training and verification procedures of the proposed NNs to summarize the mean square error (MSE) along with the LMBM. To check the efficiency, effectiveness, and correctness of the novel NSKS-EFM and the proposed SNNs-LMBM, the numerical investigations are obtainable using the comparative actions of MSE results, regression, error histograms and correlation.

1 Introduction

The singular problems arise in the mathematical engineering problems, like as inverse models, creep or viscoelasticity problems. For multi variables, the ordinary differential system has gotten much importance due to the extensive implementations in engineering and scientific and fields, e.g., chemical reactor, astrophysics, biological fields, nonlinear circuits areas, optimization of control theory, fluid dynamics, and theory of boundary layer [1–6]. The current investigations are associated to the Emden–Fowler model (EFM) that has a singularity at the origin, considered difficult and complicated to solve due to the stiffer nature. The research community always interested to solve such kinds of EFM using a variety of numerical as well as analytical schemes. The EFM has numerous submissions in engineering,

fluid dynamics, population growth system, relativistic mechanics, pattern creation system and an investigation of the chemical reactor [7–10]. The EFM is a second kind of singular mathematical model, given as [11–13]:

$$\begin{cases} D_{\tau}^{\alpha} \rho + \frac{\xi}{\tau} D_{\tau}^{\beta} \rho + g(\tau) a(\rho) = 0, & \xi \geq 1 \\ \rho(0) = \varepsilon, \quad \frac{d\rho(0)}{d\tau} = 0, \end{cases} \quad (1)$$

where $\tau = 0$ shows the singularity at the origin, ξ represents the value of the shape factor and α and β represent the order of differential terms. For $g(\tau) = 1$, the EFM takes the form of Lane–Emden system (LES), written as:

$$\begin{cases} D_{\tau}^{\alpha} \rho + \frac{\xi}{\tau} D_{\tau}^{\beta} \rho + a(\rho) = 0, & \xi \geq 1 \\ \rho(0) = \varepsilon, \quad \frac{d\rho(0)}{d\tau} = 0. \end{cases} \quad (2)$$

The LES signified in Eq. (2) presented by famous astrophysicists Lane and then explored by Emden. This celebrated historical system is applied in the model-

^a e-mail: irwan@jaincurup.ac.id

^b e-mail: mohamed.reda@bhit.bu.edu.eg (corresponding author)

ing of the temperature variational system of a gas cloud, mathematical physics, radiative cooling, stellar arrangement, polytropic star construction based on astrophysics, self-gravitating clouds of gas and the cluster galaxies modeling [14, 15]. The term $a(\rho)$ seems in numerous forms in the LES and has different forms, $a(\rho) = \rho^l$ signifies the most popular and common form, which attracted the researcher community, for $l = 0$ and 1, the LES shows a linear equation, otherwise it presents a nonlinear performance. The LES indicates the isothermal form of the gas sphere for $a(\rho) = e^\rho$. Moreover, $a(\tau)$ indicates the nonlinearity, like as $\cos u$, $\sin u$, $\sinh u$ and $\cosh u$, etc. The LES takes the form of white-dwarf system for $a(\rho) = (\rho^2 - C)^{1.5}$ accessible by Chandrasekhar [16]. The LES is implemented in density gaseous star state [17], mathematical physics system [18], electromagnetic [19], sublinear neutral span [20], oscillating magnetic systems [21], quantum mechanics model [22], isotropic-based continuous media [23] and stellar construction systems [10]. Since the invention of these models, many analytical and numerical solution techniques have been proposed to solve such singular systems. These systems having singularity are not easy to handle and only a limited existing scheme has been used to tackle such models [24–32].

To solve the singular model is also a big challenge for the research community due to the singular point and only a few analytic/numerical approaches are available to handle such systems. Few reported schemes are presented to solve the singular systems are Adomian decomposition discussed by Shawagfeh et al. [33], the series scheme is presented by Romas et al. [34], the Legendre wavelet spectral is applied by Dizicheh et al. [35], the Haar Adomian method is proposed by Saeed et al. [36], the reproduced kernel as well as group preserving approaches discussed by Hashemi et al. [37], a novel third kind of functional differential singular system using the differential transformation approach is proposed by Sabir et al [38]. The singular models have been solved by using the optimization based swarming and heuristic schemes have been provided in these references [39–42]. These are appreciated inspiration aspects to investigate in neural networks-based solver for stiff nonlinear fractional seventh order singular systems.

The aim of this work is to design a novel nonlinear fractional seventh kind of singular (NSKS) Emden–Fowler model (EFM), i.e., NSKS-EFM together with its six categories. This novel design of NSKS-EFM is obtained with the use of typical EFM of the second kind. The solution of the novel NSKS-EFM is presented numerically using the supervised neural networks (SNNs) together with the Levenberg–Marquardt backpropagation method (LMBM), i.e., SNNs-LMBM. The novel features of the present investigations are stated as follows:

- The design of a novel NSKS-EFM together with its six categories is presented using the typical EFM along with the detail of the singularity of each case along with the shape factor.

- The solution dynamics of the first category of the NSKS-EFM is presented effectively in three different cases using the stochastic procedures based on the SNNs-LMBM.
- A reference dataset using the exact solutions the first category of the novel NSKS-EFM is effectively exploiting for the creation of an approximate solution for stochastic SNNs-LMBM.
- The overlapping of the obtained numerical solutions establishes the value of the stochastic SNNs-LMBM to solve three cases based the first category of the novel NSKS-EFM.
- The SNNs-LMBM performance through comparative investigations on error histograms (EHs), correlation, regression metrics and mean square error (MSE) shows the strength of the stochastic schemes.

The rest of the parts of the paper are organized as: The structure of the novel NSKS-EFM with six groups is shown in Sect. 2. The solution of the three cases of the novel NSKS-EFM is derived in Sect. 3. The comprehensive details of the stochastic SNNs-LMBM, essential description and results of the novel NSKS-EFM through SNNs-LMBM are listed in Sect. 4. The final remarks and future research directions are listed in the final section.

2 Design of novel NSKS-EFM

This section provides the six different groups based on the novel NSKS-EFM along with the detail of shape factors and singular points for each group. The obtained novel model and its initial conditions (ICs) are achieved on the basis of typical EFM. The mathematical derivation of the novel NSKS-EFM is provided as:

$$\begin{cases} \tau^{-q_1} D_\tau^b \left(\tau^{q_1} \frac{d^c}{d\tau^c} \right) \rho_1 + g_1(\tau) f_1(\rho_1, \rho_2) = k_1(\tau), \\ \tau^{-q_2} D_\tau^b \left(\tau^{q_2} \frac{d^c}{d\tau^c} \right) \rho_2 + g_2(\tau) f_2(\rho_1, \rho_2) = k_2(\tau), \end{cases} \quad (3)$$

where q_1 and q_2 are the positive and real values, $k_1(\tau)$ and $k_2(\tau)$ are the values of forcing functions, $g_1(\tau)$ and $g_2(\tau)$ represent the function values, $f_1(\rho_1, \rho_2)$ and $f_2(\rho_1, \rho_2)$ indicate the linear/nonlinear based functions of ρ_1 and ρ_2 . For the mathematical derivation of the novel NSKS-EFM, the values of b and c must be signified as:

$$b + c = 7, \quad b, c \geq 1. \quad (4)$$

The following six possibilities satisfy the above equation as:

$$b = 6, \quad c = 1, \tag{5}$$

$$b = 5, \quad c = 2, \tag{6}$$

$$b = 4, \quad c = 3, \tag{7}$$

$$b = 3, \quad c = 4, \tag{8}$$

$$b = 2, \quad c = 5, \tag{9}$$

$$b = 1, \quad c = 6, \tag{10}$$

Type 1: The first group of the novel NSKS-EFM is achieved by using the Eqs. (5) and (3), which is written as:

$$\begin{cases} \tau^{-q_1} \frac{d^6}{d\tau^6} \left(\tau^{q_1} \frac{d}{d\tau} \right) \rho_1 + g_1(\tau)h_1(\rho_1, \rho_2) = k_1(\tau), \\ \tau^{-q_2} \frac{d^6}{d\tau^6} \left(\tau^{q_2} \frac{d}{d\tau} \right) \rho_2 + g_2(\tau)h_2(\rho_1, \rho_2) = k_2(\tau), \end{cases} \tag{11}$$

The derivatives term in the Eq. (11) is written as:

$$\begin{cases} \frac{d^6}{d\tau^6} \left(\tau^{q_1} \frac{d}{d\tau} \right) \rho_1 = \tau^{q_1} \frac{d^7 \rho_1}{d\tau^7} + 6q_1 \tau^{q_1-1} \frac{d^6 \rho_1}{d\tau^6} \\ \quad + 15q_1(q_1-1) \tau^{q_1-2} \frac{d^5 \rho_1}{d\tau^5} \\ \quad + 20q_1(q_1-1)(q_1-2) \tau^{q_1-3} \frac{d^4 \rho_1}{d\tau^4} \\ 15q_1(q_1-1)(q_1-2)(q_1-3) \tau^{q_1-4} \frac{d^3 \rho_1}{d\tau^3} \\ \quad + 6q_1(q_1-1)(q_1-2)(q_1-3)(q_1-4) \tau^{q_1-5} \frac{d^2 \rho_1}{d\tau^2} \\ \quad + q_1(q_1-1)(q_1-2)(q_1-3)(q_1-4)(q_1-5) \tau^{q_1-6} \frac{d \rho_1}{d\tau}, \\ \frac{d^6}{d\tau^6} \left(\tau^{q_2} \frac{d}{d\tau} \right) \rho_2 = \tau^{q_2} \frac{d^7 \rho_2}{d\tau^7} + 6q_2 \tau^{q_2-1} \frac{d^6 \rho_2}{d\tau^6} \\ \quad + 15q_2(q_2-1) \tau^{q_2-2} \frac{d^5 \rho_2}{d\tau^5} \\ \quad + 20q_2(q_2-1)(q_2-2) \tau^{q_2-3} \frac{d^4 \rho_2}{d\tau^4} \\ 15q_2(q_2-1)(q_2-2)(q_2-3) \tau^{q_2-4} \frac{d^3 \rho_2}{d\tau^3} \\ \quad + 6q_2(q_2-1)(q_2-2)(q_2-3)(q_2-4) \tau^{q_2-5} \frac{d^2 \rho_2}{d\tau^2} \\ \quad + q_2(q_2-1)(q_2-2)(q_2-3)(q_2-4)(q_2-5) \tau^{q_2-6} \frac{d \rho_2}{d\tau}, \end{cases} \tag{12}$$

The obtained form using the above two equations becomes as:

$$\begin{cases} \frac{d^7 \rho_1}{d\tau^7} + \frac{6q_1}{\tau} \frac{d^6 \rho_1}{d\tau^6} + \frac{15q_1(q_1-1)}{\tau^2} \frac{d^5 \rho_1}{d\tau^5} \\ \quad + \frac{20q_1(q_1-1)(q_1-2)}{\tau^3} \frac{d^4 \rho_1}{d\tau^4} \\ \quad + \frac{15q_1(q_1-1)(q_1-2)(q_1-3)}{\tau^4} \frac{d^3 \rho_1}{d\tau^3} \\ \quad + \frac{6q_1(q_1-1)(q_1-2)(q_1-3)(q_1-4)}{\tau^5} \frac{d^2 \rho_1}{d\tau^2} \\ \quad + \frac{q_1(q_1-1)(q_1-2)(q_1-3)(q_1-4)(q_1-5)}{\tau^6} \frac{d \rho_1}{d\tau} \\ \quad + g_1(\tau)h_1(\rho_1, \rho_2) = k_1(\tau), \\ \frac{d^7 \rho_2}{d\tau^7} + \frac{6q_2}{\tau} \frac{d^6 \rho_2}{d\tau^6} + \frac{15q_2(q_2-1)}{\tau^2} \frac{d^5 \rho_2}{d\tau^5} \\ \quad + \frac{20q_2(q_2-1)(q_2-2)}{\tau^3} \frac{d^4 \rho_2}{d\tau^4} \\ \quad + \frac{15q_2(q_2-1)(q_2-2)(q_2-3)}{\tau^4} \frac{d^3 \rho_2}{d\tau^3} \\ \quad + \frac{6q_2(q_2-1)(q_2-2)(q_2-3)(q_2-4)}{\tau^5} \frac{d^2 \rho_2}{d\tau^2} \\ \quad + \frac{q_2(q_2-1)(q_2-2)(q_2-3)(q_2-4)(q_2-5)}{\tau^6} \frac{d \rho_2}{d\tau} \\ \quad + g_2(\tau)h_2(\rho_1, \rho_2) = k_2(\tau), \end{cases} \tag{13}$$

The corresponding ICs for the above equation are written as:

$$\begin{cases} \rho_1(0) = I_1, \frac{d\rho_1(0)}{d\tau} = 0, \frac{d^2\rho_1(0)}{d\tau^2} = 0, \frac{d^3\rho_1(0)}{d\tau^3} = 0, \\ \frac{d^4\rho_1(0)}{d\tau^4} = 0, \frac{d^5\rho_1(0)}{d\tau^5} = 0, \frac{d^6\rho_1(0)}{d\tau^6} = 0 \\ \rho_2(0) = I_2, \frac{d\rho_2(0)}{d\tau} = 0, \frac{d^2\rho_2(0)}{d\tau^2} = 0, \frac{d^3\rho_2(0)}{d\tau^3} = 0, \\ \frac{d^4\rho_2(0)}{d\tau^4} = 0, \frac{d^5\rho_2(0)}{d\tau^5} = 0, \frac{d^6\rho_2(0)}{d\tau^6} = 0 \end{cases} \tag{14}$$

The achieved form of above two equations represents the multiple singular points, nonlinear forms, fractional seventh order along with the differential equation system. The singularity at $\tau = 0$ appears six times for both the parameters $\rho_1(\tau)$ and $\rho_2(\tau)$, respectively. The shape factor values are $6q_1, 15q_1(q_1 - 1), 20q_1(q_1 - 1)(q_1 - 2), 15q_1(q_1 - 1)(q_1 - 2)(q_1 - 3), 6q_1(q_1 - 1)(q_1 - 2)(q_1 - 3)(q_1 - 4)$ and $q_1(q_1 - 1)(q_1 - 2)(q_1 - 3)(q_1 - 4)(q_1 - 5)$ for $\rho_1(\tau)$, while for $\rho_2(\tau)$, the shape factors is $6q_2, 15q_2(q_2 - 1), 20q_2(q_2 - 1)(q_2 - 2), 15q_2(q_2 - 1)(q_2 - 2)(q_2 - 3), 6q_2(q_2 - 1)(q_2 - 2)(q_2 - 3)(q_2 - 4)$ and $q_2(q_2 - 1)(q_2 - 2)(q_2 - 3)(q_2 - 4)(q_2 - 5)$, respectively. It is noted for $q_1 = q_2 = 1$, the third, fourth, fifth, sixth and seventh expressions vanish for the $\rho_1(\tau)$ and $\rho_2(\tau)$ parameters and the shape factor values reduces to 6. For $q_1 = q_2 = 2$ the fourth, fifth, sixth and seventh expressions vanish for the $\rho_1(\tau)$ and $\rho_2(\tau)$ parameters and the shape factor values reduces to 12 and 30, respectively. For $q_1 = q_2 = 3$, the fifth, sixth and seventh expressions vanish for the $\rho_1(\tau)$ and $\rho_2(\tau)$ parameters and the shape factor values reduces to 18, 90 and 120, respectively. Similarly, for $q_1 = q_2 = 4$, the sixth and seventh expressions vanish for the $\rho_1(\tau)$ and $\rho_2(\tau)$ parameters and the shape factor values reduces to 24, 180, 480 and 360, respectively. Moreover, for $q_1 = q_2 = 5$, the seventh expression vanishes for the $\rho_1(\tau)$ and $\rho_2(\tau)$ parameters and the shape factor values reduces to 30, 300, 1200, 1800 and 720, respectively.

Type 2: The second group of the novel NSKS-EFM is achieved by using the Eqs. (3) and (6), which is written as:

$$\begin{cases} \tau^{-q_1} \frac{d^5}{d\tau^5} \left(\tau^{q_1} \frac{d^2}{d\tau^2} \right) \rho_1 + g_1(\tau)f_1(\rho_1, \rho_2) = k_1(\tau), \\ \tau^{-q_2} \frac{d^5}{d\tau^5} \left(\tau^{q_2} \frac{d^2}{d\tau^2} \right) \rho_2 + g_2(\tau)f_2(\rho_1, \rho_2) = k_2(\tau), \end{cases} \tag{15}$$

The derivatives term in the Eq. (15) is written as:

$$\left\{ \begin{aligned} & \frac{d^5}{d\tau^5} \left(\tau^{q_1} \frac{d^2}{d\tau^2} \right) \rho_1 = 5\tau^{q_1} \frac{d^6 \rho_1}{d\tau^6} + 10q_1 \tau^{q_1-1} \frac{d^5 \rho_1}{d\tau^5} \\ & + 10q_1(q_1-1) \tau^{q_1-2} \frac{d^4 \rho_1}{d\tau^4} \\ & + 5q_1(q_1-1)(q_1-2) \tau^{q_1-3} \frac{d^3 \rho_1}{d\tau^3} \\ & + q_1(q_1-1)(q_1-2)(q_1-3) \tau^{q_1-4} \frac{d^2 \rho_1}{d\tau^2}, \\ & \frac{d^5}{d\tau^5} \left(\tau^{q_2} \frac{d^2}{d\tau^2} \right) \rho_2 = 5\tau^{q_2} \frac{d^6 \rho_2}{d\tau^6} + 10q_2 \tau^{q_2-1} \frac{d^5 \rho_2}{d\tau^5} \\ & + 10q_2(q_2-1) \tau^{q_2-2} \frac{d^4 \rho_2}{d\tau^4} + \\ & 5q_2(q_2-1)(q_2-2) \tau^{q_2-3} \frac{d^3 \rho_2}{d\tau^3} \\ & + q_2(q_2-1)(q_2-2)(q_2-3) \tau^{q_2-4} \frac{d^2 \rho_2}{d\tau^2}, \end{aligned} \right. \tag{16}$$

The obtained mathematical form using the above two equations becomes as:

$$\left\{ \begin{aligned} & \frac{d^7 \rho_1}{d\tau^7} + \frac{5q_1}{\tau} \frac{d^6 \rho_1}{d\tau^6} + \frac{10q_1(q_1-1)}{\tau^2} \frac{d^5 \rho_1}{d\tau^5} \\ & + \frac{10q_1(q_1-1)(q_1-2)}{\tau^3} \frac{d^4 \rho_1}{d\tau^4} \\ & + \frac{5q_1(q_1-1)(q_1-2)(q_1-3)}{\tau^4} \frac{d^3 \rho_1}{d\tau^3} \\ & + \frac{q_1(q_1-1)(q_1-2)(q_1-3)(q_1-4)}{\tau^5} \frac{d^2 \rho_1}{d\tau^2} \\ & + g_1(\tau) h_1(\rho_1, \rho_2) = k_1(\tau), \\ & \frac{d^7 \rho_2}{d\tau^7} + \frac{5q_2}{\tau} \frac{d^6 \rho_2}{d\tau^6} + \frac{10q_2(q_2-1)}{\tau^2} \frac{d^5 \rho_2}{d\tau^5} \\ & + \frac{10q_2(q_2-1)(q_2-2)}{\tau^3} \frac{d^4 \rho_2}{d\tau^4} \\ & + \frac{5q_2(q_2-1)(q_2-2)(q_2-3)}{\tau^4} \frac{d^3 \rho_2}{d\tau^3} \\ & + \frac{q_2(q_2-1)(q_2-2)(q_2-3)(q_2-4)}{\tau^5} \frac{d^2 \rho_2}{d\tau^2} \\ & + g_2(\tau) h_2(\rho_1, \rho_2) = k_2(\tau), \end{aligned} \right. \tag{17}$$

The corresponding ICs for the above equation are written as:

$$\left\{ \begin{aligned} & \rho_1(0) = I_1, \frac{d\rho_1(0)}{d\tau} = I_3, \frac{d^2 \rho_1(0)}{d\tau^2} = 0, \frac{d^3 \rho_1(0)}{d\tau^3} = 0, \\ & \frac{d^4 \rho_1(0)}{d\tau^4} = 0, \frac{d^5 \rho_1(0)}{d\tau^5} = 0, \frac{d^6 \rho_1(0)}{d\tau^6} = 0, \\ & \rho_2(0) = I_2, \frac{d\rho_2(0)}{d\tau} = I_4, \frac{d^2 \rho_2(0)}{d\tau^2} = 0, \frac{d^3 \rho_2(0)}{d\tau^3} = 0, \\ & \frac{d^4 \rho_2(0)}{d\tau^4} = 0, \frac{d^5 \rho_2(0)}{d\tau^5} = 0, \frac{d^6 \rho_2(0)}{d\tau^6} = 0. \end{aligned} \right. \tag{18}$$

The achieved form of above two equations represents the multiple singular points, nonlinear forms, fractional seventh order along with the differential equations system. The singularity at $\tau = 0$ appears five times for both the parameters $\rho_1(\tau)$ and $\rho_2(\tau)$, respectively. The shape factor values are $5q_1, 10q_1(q_1 - 1), 10q_1(q_1 - 1)(q_1 - 2), 5q_1(q_1 - 1)(q_1 - 2)(q_1 - 3)$ and $q_1(q_1 - 1)(q_1 - 2)(q_1 - 3)(q_1 - 4)$ for $\rho_1(\tau)$, whereas for the $\rho_2(\tau)$ parameter, the values of the shape factors are $5q_2, 10q_2(q_2 - 1), 10q_2(q_2 - 1)(q_2 - 2), 5q_2(q_2 - 1)(q_2 - 2)(q_2 - 3)$ and $q_2(q_2 - 1)(q_2 - 2)(q_2 - 3)(q_2 - 4)$, respectively. It is noted

for $q_1 = q_2 = 1$, the third, fourth, fifth and sixth expressions vanish for the $\rho_1(\tau)$ and $\rho_2(\tau)$ parameters and the shape factor values reduces to 5. For $q_1 = q_2 = 2$, the fourth, fifth and sixth expressions vanish for the $\rho_1(\tau)$ and $\rho_2(\tau)$ parameters and the shape factor values reduces to 10 and 20, respectively. For $q_1 = q_2 = 3$, the fifth and sixth expressions vanish for the $\rho_1(\tau)$ and $\rho_2(\tau)$ parameters and the shape factor values reduces to 15, 60 and 60, respectively. Similarly, for $q_1 = q_2 = 4$, the sixth expressions vanish for the $\rho_1(\tau)$ and $\rho_2(\tau)$ parameters and the shape factor values reduces to 20, 120, 240 and 120, respectively.

Type 3: The third group of the novel NSKS-EFM is achieved by using the Eqs. (3) and (7), which is written as:

$$\left\{ \begin{aligned} & \tau^{-q_1} \frac{d^4}{d\tau^4} \left(\tau^{q_1} \frac{d^3}{d\tau^3} \right) \rho_1 + g_1(\tau) f_1(\rho_1, \rho_2) = k_1(\tau), \\ & \tau^{-q_2} \frac{d^4}{d\tau^4} \left(\tau^{q_2} \frac{d^3}{d\tau^3} \right) \rho_2 + g_2(\tau) f_2(\rho_1, \rho_2) = k_2(\tau), \end{aligned} \right. \tag{19}$$

The derivatives term in the Eq. (19) is written as:

$$\left\{ \begin{aligned} & \frac{d^4}{d\tau^4} \left(\tau^{q_1} \frac{d^3}{d\tau^3} \right) \rho_1 = \tau^{q_1} \frac{d^7 \rho_1}{d\tau^7} + 4q_1 \tau^{q_1-1} \frac{d^6 \rho_1}{d\tau^6} \\ & + 6q_1(q_1-1) \tau^{q_1-2} \frac{d^5 \rho_1}{d\tau^5} \\ & + 4q_1(q_1-1)(q_1-2) \tau^{q_1-3} \frac{d^4 \rho_1}{d\tau^4} \\ & + q_1(q_1-1)(q_1-2)(q_1-3) \tau^{q_1-4} \frac{d^3 \rho_1}{d\tau^3}, \\ & \frac{d^4}{d\tau^4} \left(\tau^{q_2} \frac{d^3}{d\tau^3} \right) \rho_2 = \tau^{q_2} \frac{d^7 \rho_2}{d\tau^7} + 4q_2 \tau^{q_2-1} \frac{d^6 \rho_2}{d\tau^6} \\ & + 6q_2(q_2-1) \tau^{q_2-2} \frac{d^5 \rho_2}{d\tau^5} \\ & + 4q_2(q_2-1)(q_2-2) \tau^{q_2-3} \frac{d^4 \rho_2}{d\tau^4} \\ & + q_2(q_2-1)(q_2-2)(q_2-3) \tau^{q_2-4} \frac{d^3 \rho_2}{d\tau^3}, \end{aligned} \right. \tag{20}$$

The obtained mathematical form using the above two equations is becomes as:

$$\left\{ \begin{aligned} & \frac{d^7 \rho_1}{d\tau^7} + \frac{4q_1}{\tau} \frac{d^6 \rho_1}{d\tau^6} + \frac{6q_1(q_1-1)}{\tau^2} \frac{d^5 \rho_1}{d\tau^5} + \frac{4q_1(q_1-1)(q_1-2)}{\tau^3} \frac{d^4 \rho_1}{d\tau^4} \\ & + \frac{q_1(q_1-1)(q_1-2)(q_1-3)}{\tau^4} \frac{d^3 \rho_1}{d\tau^3} + g_1(\tau) h_1(\rho_1, \rho_2) = k_1(\tau), \\ & \frac{d^7 \rho_2}{d\tau^7} + \frac{4q_2}{\tau} \frac{d^6 \rho_2}{d\tau^6} + \frac{6q_2(q_2-1)}{\tau^2} \frac{d^5 \rho_2}{d\tau^5} + \frac{4q_2(q_2-1)(q_2-2)}{\tau^3} \frac{d^4 \rho_2}{d\tau^4} + \\ & \frac{q_2(q_2-1)(q_2-2)(q_2-3)}{\tau^4} \frac{d^3 \rho_2}{d\tau^3} + g_2(\tau) h_2(\rho_1, \rho_2) = k_2(\tau), \end{aligned} \right. \tag{21}$$

The corresponding ICs for the above equation are written as:

$$\left\{ \begin{aligned} & \rho_1(0) = I_1, \frac{d\rho_1(0)}{d\tau} = I_3, \frac{d^2 \rho_1(0)}{d\tau^2} = I_5, \frac{d^3 \rho_1(0)}{d\tau^3} = 0, \\ & \frac{d^4 \rho_1(0)}{d\tau^4} = 0, \frac{d^5 \rho_1(0)}{d\tau^5} = 0, \frac{d^6 \rho_1(0)}{d\tau^6} = 0, \\ & \rho_2(0) = I_2, \frac{d\rho_2(0)}{d\tau} = I_4, \frac{d^2 \rho_2(0)}{d\tau^2} = I_6, \frac{d^3 \rho_2(0)}{d\tau^3} = 0, \\ & \frac{d^4 \rho_2(0)}{d\tau^4} = 0, \frac{d^5 \rho_2(0)}{d\tau^5} = 0, \frac{d^6 \rho_2(0)}{d\tau^6} = 0. \end{aligned} \right. \tag{22}$$

The achieved mathematical form of above two equations represents the multiple singular points, nonlinear

forms, fractional seventh order along with the differential equations system. The singularity at $\tau = 0$ appears four times for both the parameters $\rho_1(\tau)$ and $\rho_2(\tau)$, respectively. The shape factor values are $4q_1, 6q_1(q_1 - 1), 4q_1(q_1 - 1)(q_1 - 2)$ and $q_1(q_1 - 1)(q_1 - 2)(q_1 - 3)$, for $\rho_1(\tau)$, whereas for the $\rho_2(\tau)$ parameter, the values of the shape factors are $4q_2, 6q_2(q_2 - 1), 4q_2(q_2 - 1)(q_2 - 2)$ and $q_2(q_2 - 1)(q_2 - 2)(q_2 - 3)$, respectively. It is noted that for $q_1 = q_2 = 1$, the third, fourth and fifth terms vanish for the parameters $\rho_1(\tau)$ and $\rho_2(\tau)$, the shape factors for $\rho_1(\tau)$ and $\rho_2(\tau)$ reduces to 4. For $q_1 = q_2 = 2$, the fourth and fifth terms vanish for $\rho_1(\tau)$ and $\rho_2(\tau)$, while the shape factor for both of the parameters $\rho_1(\tau)$ and $\rho_2(\tau)$ reduces to 8 and 12, respectively. Similarly, for $q_1 = q_2 = 3$, the fifth expressions vanish for the $\rho_1(\tau)$ and $\rho_2(\tau)$, while the shape factor values reduces to 12, 36 and 24, respectively.

Type 4: The fourth group of the novel NSKS-EFM is achieved by using the Eqs. (3) and (8), which is written as:

$$\begin{cases} \tau^{-q_1} \frac{d^3}{d\tau^3} \left(\tau^{q_1} \frac{d^4}{d\tau^4} \right) \rho_1 + g_1(\tau) f_1(\rho_1, \rho_2) = k_1(\tau), \\ \tau^{-q_2} \frac{d^3}{d\tau^3} \left(\tau^{q_2} \frac{d^4}{d\tau^4} \right) \rho_2 + g_2(\tau) f_2(\rho_1, \rho_2) = k_2(\tau), \end{cases} \tag{23}$$

The derivatives term in the Eq. (23) is written as:

$$\begin{cases} \frac{d^3}{d\tau^3} \left(\tau^{q_1} \frac{d^4}{d\tau^4} \right) \rho_1 = \tau^{q_1} \frac{d^7 \rho_1}{d\tau^7} + 3q_1 \tau^{q_1-1} \frac{d^6 \rho_1}{d\tau^6} \\ \quad + 3q_1(q_1 - 1) \tau^{q_1-2} \frac{d^5 \rho_1}{d\tau^5} \\ \quad + q_1(q_1 - 1)(q_1 - 2) \tau^{q_1-3} \frac{d^4 \rho_1}{d\tau^4}, \\ \frac{d^3}{d\tau^3} \left(\tau^{q_2} \frac{d^4}{d\tau^4} \right) \rho_2 = \tau^{q_2} \frac{d^7 \rho_2}{d\tau^7} + 3q_2 \tau^{q_2-1} \frac{d^6 \rho_2}{d\tau^6} \\ \quad + 3q_2(q_2 - 1) \tau^{q_2-2} \frac{d^5 \rho_2}{d\tau^5} \\ \quad + q_2(q_2 - 1)(q_2 - 2) \tau^{q_2-3} \frac{d^4 \rho_2}{d\tau^4}, \end{cases} \tag{24}$$

The obtained mathematical form using the above two equations is becomes as:

$$\begin{cases} \frac{d^7 \rho_1}{d\tau^7} + \frac{3q_1}{\tau} \frac{d^6 \rho_1}{d\tau^6} + \frac{3q_1(q_1-1)}{\tau^2} \frac{d^5 \rho_1}{d\tau^5} \\ \quad + \frac{q_1(q_1-1)(q_1-2)}{\tau^3} \frac{d^4 \rho_1}{d\tau^4} + g_1(\tau) h_1(\rho_1, \rho_2) = k_1(\tau), \\ \frac{d^7 \rho_2}{d\tau^7} + \frac{3q_2}{\tau} \frac{d^6 \rho_2}{d\tau^6} + \frac{3q_2(q_2-1)}{\tau^2} \frac{d^5 \rho_2}{d\tau^5} \\ \quad + \frac{q_2(q_2-1)(q_2-2)}{\tau^3} \frac{d^4 \rho_2}{d\tau^4} + g_2(\tau) h_2(\rho_1, \rho_2) = k_2(\tau), \end{cases} \tag{25}$$

The corresponding ICs for the above equation are written as:

$$\begin{cases} \rho_1(0) = I_1, \frac{d\rho_1(0)}{d\tau} = I_3, \frac{d^2\rho_1(0)}{d\tau^2} = I_5, \frac{d^3\rho_1(0)}{d\tau^3} = I_7, \\ \frac{d^4\rho_1(0)}{d\tau^4} = \frac{d^5\rho_1(0)}{d\tau^5} = \frac{d^6\rho_1(0)}{d\tau^6} = 0, \\ \rho_2(0) = I_2, \frac{d\rho_2(0)}{d\tau} = I_4, \frac{d^2\rho_2(0)}{d\tau^2} = I_6, \frac{d^3\rho_2(0)}{d\tau^3} = I_8, \\ \frac{d^4\rho_2(0)}{d\tau^4} = \frac{d^5\rho_2(0)}{d\tau^5} = \frac{d^6\rho_2(0)}{d\tau^6} = 0. \end{cases} \tag{26}$$

The achieved mathematical form of above two equations represents the multiple singular points, nonlinear forms, fractional seventh order along with the differential equations system. The singularity at $\tau = 0$ appears three times for both the parameters $\rho_1(\tau)$ and $\rho_2(\tau)$, respectively. The shape factor values are $3q_1, 3q_1(q_1 - 1)$ and $q_1(q_1 - 1)(q_1 - 2)$ for $\rho_1(\tau)$, while for the $\rho_2(\tau)$ parameter, the shape factors is $3q_2, 3q_2(q_2 - 1)$ and $q_2(q_2 - 1)(q_2 - 2)$, respectively. It is noted that for $q_1 = q_2 = 1$, the third and fourth expressions for the $\rho_1(\tau)$ and $\rho_2(\tau)$ vanish, while the values of the shape factor $\rho_1(\tau)$ and $\rho_2(\tau)$ reduces to 3. For $q_1 = q_2 = 2$, the fourth term vanishes for $\rho_1(\tau)$ and $\rho_2(\tau)$, while the shape factor for both of the parameters $\rho_1(\tau)$ and $\rho_2(\tau)$ reduces to 6 and 6, respectively.

Type 5: The fifth group of the novel NSKS-EFM is achieved by using the Eqs. (3) and (8), which is written as:

$$\begin{cases} \tau^{-q_1} \frac{d^2}{d\tau^2} \left(\tau^{q_1} \frac{d^5}{d\tau^5} \right) \rho_1 + g_1(\tau) f_1(\rho_1, \rho_2) = k_1(\tau), \\ \tau^{-q_2} \frac{d^2}{d\tau^2} \left(\tau^{q_2} \frac{d^5}{d\tau^5} \right) \rho_2 + g_2(\tau) f_2(\rho_1, \rho_2) = k_2(\tau), \end{cases} \tag{27}$$

The derivatives term in the Eq. (27) is written as:

$$\begin{cases} \frac{d^2}{d\tau^2} \left(\tau^{q_1} \frac{d^5}{d\tau^5} \right) \rho_1 = \tau^{q_1} \frac{d^7 \rho_1}{d\tau^7} + 2q_1 \tau^{q_1-1} \frac{d^6 \rho_1}{d\tau^6} \\ \quad + q_1(q_1 - 1) \tau^{q_1-2} \frac{d^5 \rho_1}{d\tau^5}, \\ \frac{d^2}{d\tau^2} \left(\tau^{q_2} \frac{d^5}{d\tau^5} \right) \rho_2 = \tau^{q_2} \frac{d^7 \rho_2}{d\tau^7} + 2q_2 \tau^{q_2-1} \frac{d^6 \rho_2}{d\tau^6} \\ \quad + q_2(q_2 - 1) \tau^{q_2-2} \frac{d^5 \rho_2}{d\tau^5}, \end{cases} \tag{28}$$

The obtained mathematical form using the above two equations is becomes as:

$$\begin{cases} \frac{d^7 \rho_1}{d\tau^7} + \frac{2q_1}{\tau} \frac{d^6 \rho_1}{d\tau^6} + \frac{q_1(q_1-1)}{\tau^2} \frac{d^5 \rho_1}{d\tau^5} \\ \quad + g_1(\tau) h_1(\rho_1, \rho_2) = k_1(\tau), \\ \frac{d^7 \rho_2}{d\tau^7} + \frac{2q_2}{\tau} \frac{d^6 \rho_2}{d\tau^6} + \frac{q_2(q_2-1)}{\tau^2} \frac{d^5 \rho_2}{d\tau^5} \\ \quad + g_2(\tau) h_2(\rho_1, \rho_2) = k_2(\tau), \end{cases} \tag{29}$$

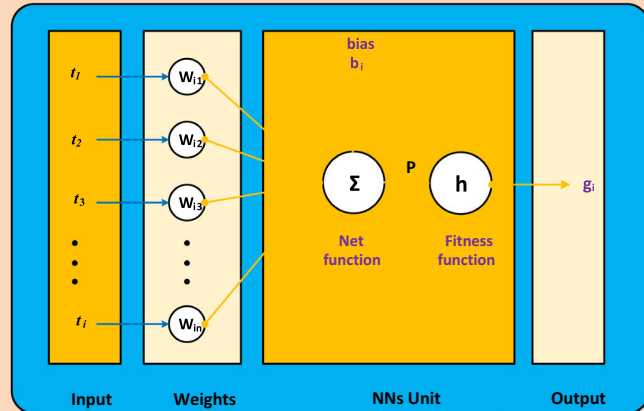
1. Methodology

Reference dataset

Proposed dataset based on the exact solutions for solving the novel NSKS-EFM

Intelligent computing

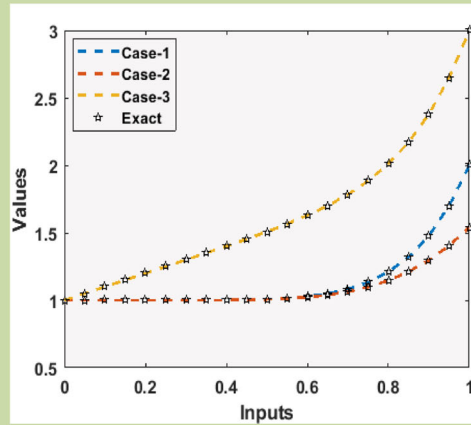
Multi-layer organization based on the SNNs-LMBM



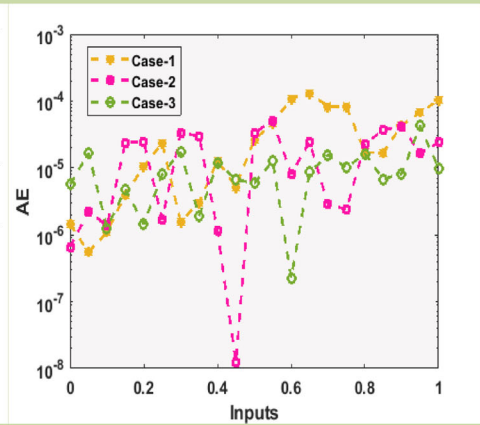
Neuron Model

2. Results Simulations

Result comparison of the SNNs-LMBM with reference dataset along with the AE for each case of the novel NSKS-EFM



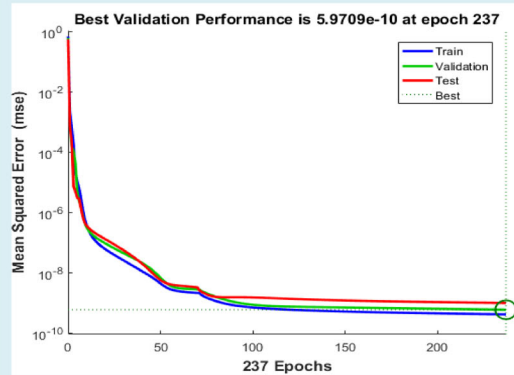
Result Comparison



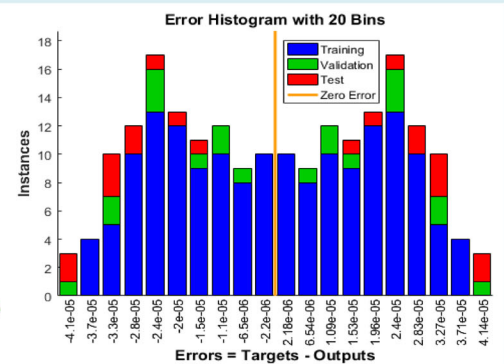
AE

3. Results analysis

Proposed solutions of the SNNs-LMBM using the MSE, Regression plots, Fitness, State transition and EHs for solving the novel NSKS-EFM



Performance



EHS

Fig. 1 Workflow illustrations using the SNNs-LMBM for solving the novel NSKS-EFM

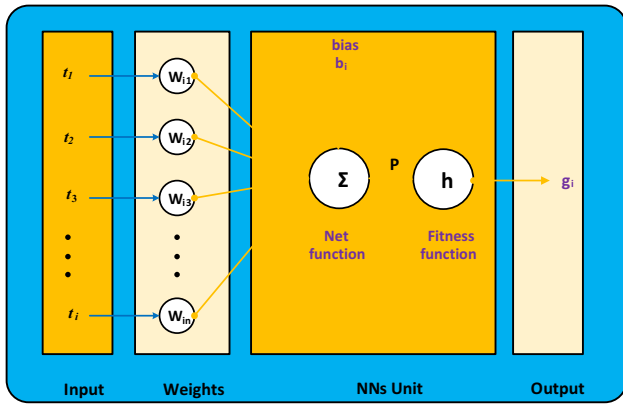


Fig. 2 Designed network using the structure of single neurons

The corresponding ICs for the above equation are written as:

$$\begin{cases} \rho_1(0) = I_1, \frac{d\rho_1(0)}{d\tau} = I_3, \frac{d^2\rho_1(0)}{d\tau^2} = I_5, \frac{d^3\rho_1(0)}{d\tau^3} = I_7, \\ \frac{d^4\rho_1(0)}{d\tau^4} = I_9, \frac{d^5\rho_1(0)}{d\tau^5} = \frac{d^6\rho_1(0)}{d\tau^6} = 0, \\ \rho_2(0) = I_2, \frac{d\rho_2(0)}{d\tau} = I_4, \frac{d^2\rho_2(0)}{d\tau^2} = I_6, \frac{d^3\rho_2(0)}{d\tau^3} = I_8, \\ \frac{d^4\rho_2(0)}{d\tau^4} = I_{10}, \frac{d^5\rho_2(0)}{d\tau^5} = \frac{d^6\rho_2(0)}{d\tau^6} = 0. \end{cases} \quad (30)$$

The achieved mathematical form of above two equations represents the multiple singular points, nonlinear forms, fractional seventh order along with the differential equations system. The singularity at $\tau = 0$ appears twice for both the parameters $\rho_1(\tau)$ and $\rho_2(\tau)$, respectively. The singularity appears twice at $\tau = 0$ for the $\rho_1(\tau)$ and $\rho_2(\tau)$, respectively. The shape factor values are $2q_1$ and $q_1(q_1 - 1)$ for $\rho_1(\tau)$, while, for the $\rho_2(\tau)$ parameter, the shape factor are $2q_2$ and $q_2(q_2 - 1)$, respectively.

Type 6: The sixth group of the novel NSKS-EFM is achieved by using the Eqs. (3) and (8), which is written as:

$$\begin{cases} \tau^{-q_1} \frac{d}{d\tau} \left(\tau^{q_1} \frac{d^6}{d\tau^6} \right) \rho_1 + g_1(\tau) f_1(\rho_1, \rho_2) = k_1(\tau), \\ \tau^{-q_2} \frac{d}{d\tau} \left(\tau^{q_2} \frac{d^6}{d\tau^6} \right) \rho_2 + g_2(\tau) f_2(\rho_1, \rho_2) = k_2(\tau), \end{cases} \quad (31)$$

The obtained mathematical form using the above two equations is becomes as:

$$\begin{cases} \frac{d}{d\tau} \left(\tau^{q_1} \frac{d^6}{d\tau^6} \right) \rho_1 = \tau^{q_1} \frac{d^7 \rho_1}{d\tau^7} + q_1 \tau^{q_1-1} \frac{d^6 \rho_1}{d\tau^6}, \\ \frac{d}{d\tau} \left(\tau^{q_2} \frac{d^6}{d\tau^6} \right) \rho_2 = \tau^{q_2} \frac{d^7 \rho_2}{d\tau^7} + q_2 \tau^{q_2-1} \frac{d^6 \rho_2}{d\tau^6}, \end{cases} \quad (32)$$

The obtained mathematical form using the above two equations is becomes as:

$$\begin{cases} \frac{d^7 \rho_1}{d\tau^7} + \frac{q_1}{\tau} \frac{d^6 \rho_1}{d\tau^6} + g_1(\tau) h_1(\rho_1, \rho_2) = k_1(\tau), \\ \frac{d^7 \rho_2}{d\tau^7} + \frac{q_2}{\tau} \frac{d^6 \rho_2}{d\tau^6} + g_2(\tau) h_2(\rho_1, \rho_2) = k_2(\tau), \end{cases} \quad (33)$$

The corresponding ICs for the above equation are written as:

$$\begin{cases} \rho_1 = I_1, \frac{d\rho_1}{d\tau} = I_3, \frac{d^2\rho_1}{d\tau^2} = I_5, \frac{d^3\rho_1}{d\tau^3} = I_7, \frac{d^4\rho_1}{d\tau^4} = I_9, \\ \frac{d^5\rho_1}{d\tau^5} = I_{11}, \frac{d^6\rho_1}{d\tau^6} = 0, \\ \rho_2 = I_2, \frac{d\rho_2}{d\tau} = I_4, \frac{d^2\rho_2}{d\tau^2} = I_6, \frac{d^3\rho_2}{d\tau^3} = I_8, \frac{d^4\rho_2}{d\tau^4} = I_{10}, \\ \frac{d^5\rho_2}{d\tau^5} = I_{12}, \frac{d^6\rho_2}{d\tau^6} = 0. \end{cases} \quad (34)$$

at $\tau \rightarrow 0$

The achieved mathematical form of above two equations represents the multiple singular points, nonlinear forms, fractional seventh order along with the differential equations system. The singularity at $\tau = 0$ appears single time for both the parameters $\rho_1(\tau)$ and $\rho_2(\tau)$, respectively. The singularity at $\tau = 0$ shows one time for the $\rho_1(\tau)$ and $\rho_2(\tau)$, respectively. The shape factor values are q_1 and q_2 for the parameters $\rho_1(\tau)$ and $\rho_2(\tau)$, respectively.

3 Methodology

In this section, the designed methodology for solving the novel NSKS-EFM is structured in two steps; first, necessary descriptions are provided to get the reference dataset for the designed SNNs-LMBM. Secondly, the implementation procedures for the designed SNNs-LMBM are described. The workflow illustrations are defined in Fig. 1. The reference dataset based on the exact solutions is proposed to check the comparison of the obtained results. The proposed SNNs-LMBM is the combination of the multi-layer SNNs along with the optimization procedures of the LMBM. Figure 2 demonstrates a system of a single neuron in the SNNs system, while the SNNs-LMBM is implemented using the 'nftool' routine of NNs in the "Matlab" using the training, testing and validation data, appropriate setting of the hidden neurons and learning methodology.

4 Results and discussions

This section shows the three different cases of type 1 based on the novel NSKS-EFM. The numerical solutions using the proposed SNNs-LMBM have been provided. The obtained form of the numerical outcomes based on the SNNs-LMBM are considered in the input $[0, 1]$ with the step size of 0.01 for solving the novel NSKS-EFM. The proposed SNNs-LMBM is executed

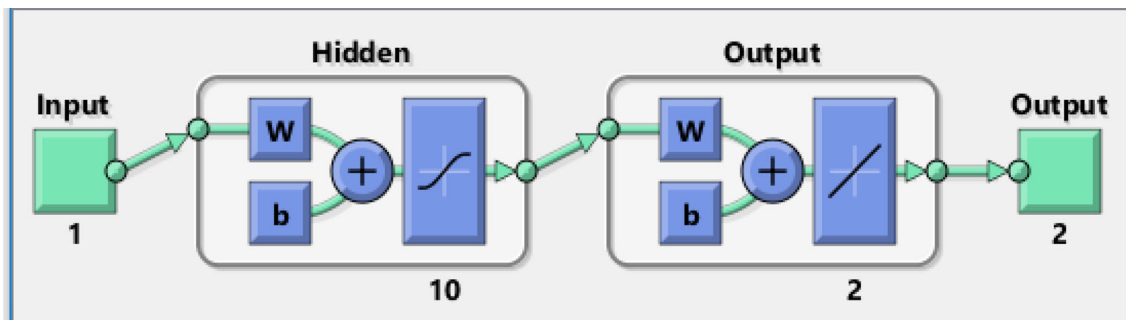


Fig. 3 Designed framework of the SNNs-LMBM for solving the novel NSKS-EFM

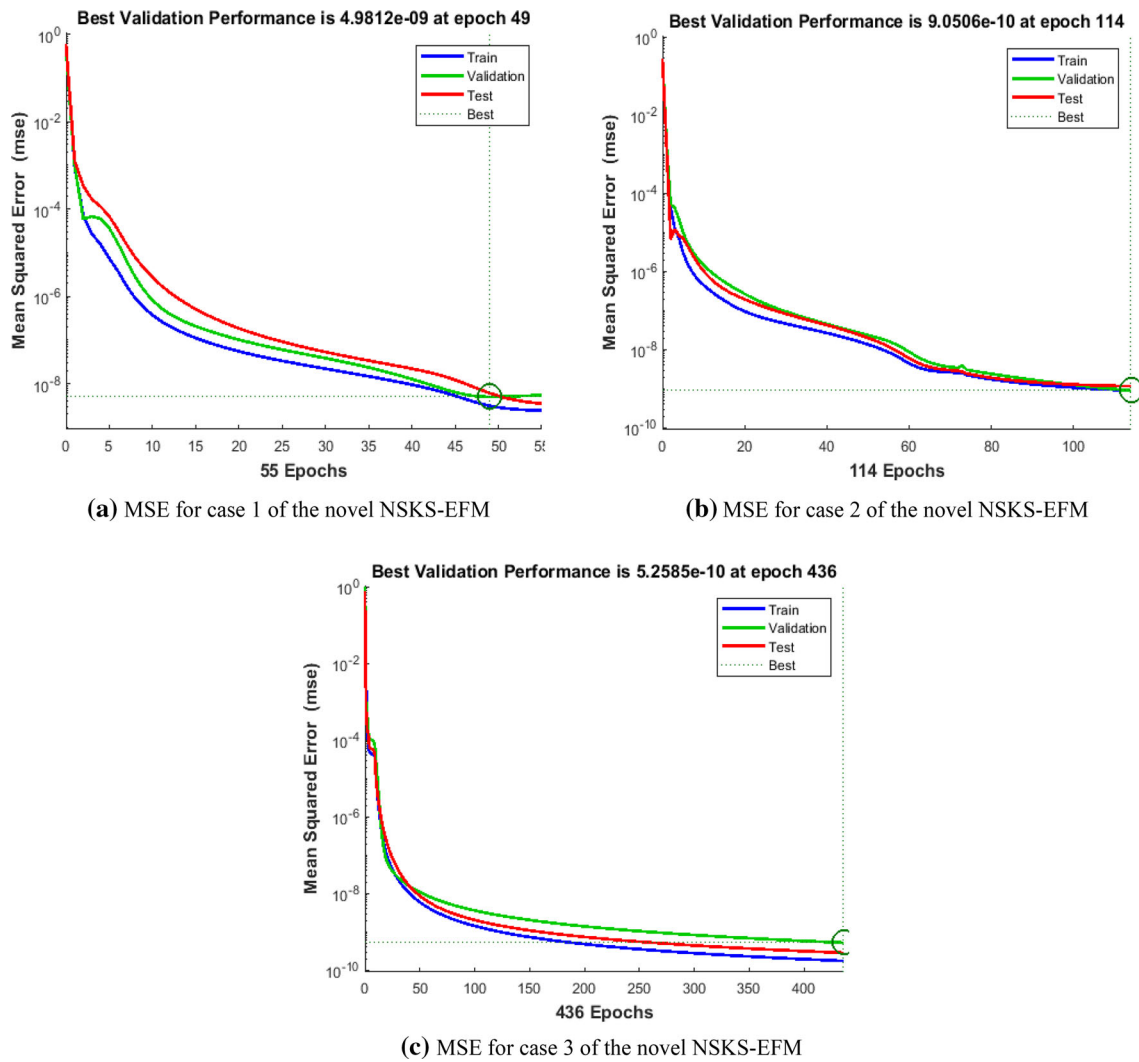


Fig. 4 Performance curves using the MSE values based on the proposed SNNs-LMBM for solving the novel NSKS-EFM

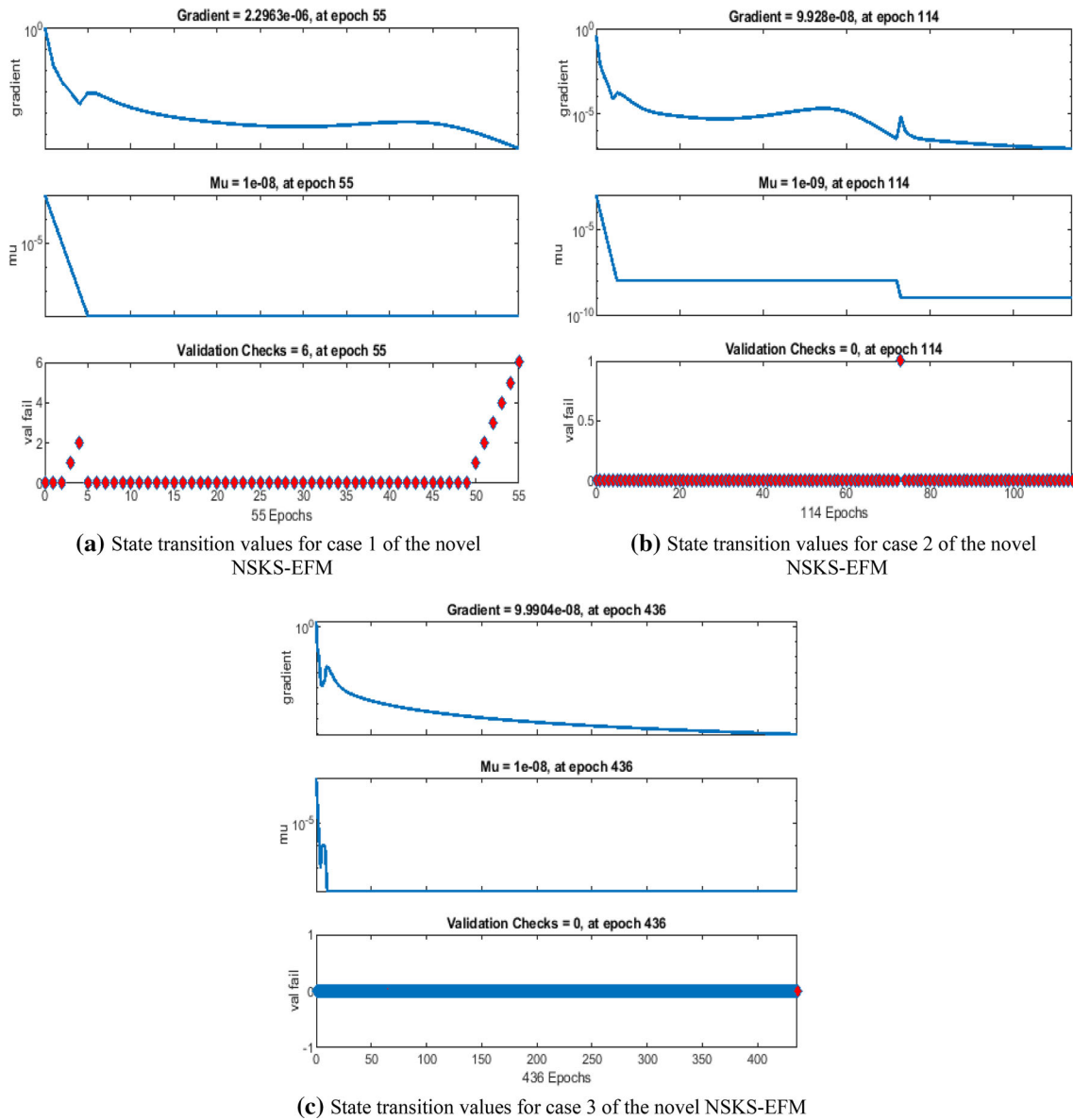


Fig. 5 State transition values for the proposed SNNs-LMBM to solve case 1, 2 and 3 of the novel NSKS-EFM

to solve each case of the novel NSKS-EFM using the routine of ‘nftool’ in “Matlab” with 10 numbers of hidden layers, 80% of training and validation/testing data is 10% for the optimization procedures of SNNs-LMBM. The proposed SNNs-LMBM is illustrated in Fig 3, however, the SNNs-LMBM is proficient to solve each type of the novel NSKS-EFM.

4.1 NSKS-EFM of type 1

In this type, three different cases of type 1 based on the novel NSKS-EFM will be derived. These proposed model-based nonlinear equations are obtained for the values of $q_1 = q_2 = 6$ in the system (13).

Case 1: Consider the singular system based on the NSKS-EFM is written as:

$$\begin{cases}
 \frac{d^7 \rho_1}{d\tau^7} + \frac{36}{\tau} \frac{d^6 \rho_1}{d\tau^6} + \frac{450}{\tau^2} \frac{d^5 \rho_1}{d\tau^5} + \frac{2400}{\tau^3} \frac{d^4 \rho_1}{d\tau^4} + \frac{4500}{\tau^4} \frac{d^3 \rho_1}{d\tau^3} \\
 + \frac{4320}{\tau^5} \frac{d^2 \rho_1}{d\tau^2} + \frac{720}{\tau^6} \frac{d\rho_1}{d\tau} + \rho_1^2 \rho_2 \\
 = 4656961 + \tau^7 - \tau^{14} - \tau^{21}, \\
 \frac{d^7 \rho_2}{d\tau^7} + \frac{36}{\tau} \frac{d^6 \rho_2}{d\tau^6} + \frac{450}{\tau^2} \frac{d^5 \rho_2}{d\tau^5} + \frac{2400}{\tau^3} \frac{d^4 \rho_2}{d\tau^4} + \frac{4500}{\tau^4} \frac{d^3 \rho_2}{d\tau^3} \\
 + \frac{4320}{\tau^5} \frac{d^2 \rho_2}{d\tau^2} + \frac{720}{\tau^6} \frac{d\rho_2}{d\tau} + \rho_1 \rho_2^2 \\
 = -4656959 - \tau^7 - \tau^{14} + \tau^{21},
 \end{cases}
 \tag{35}$$

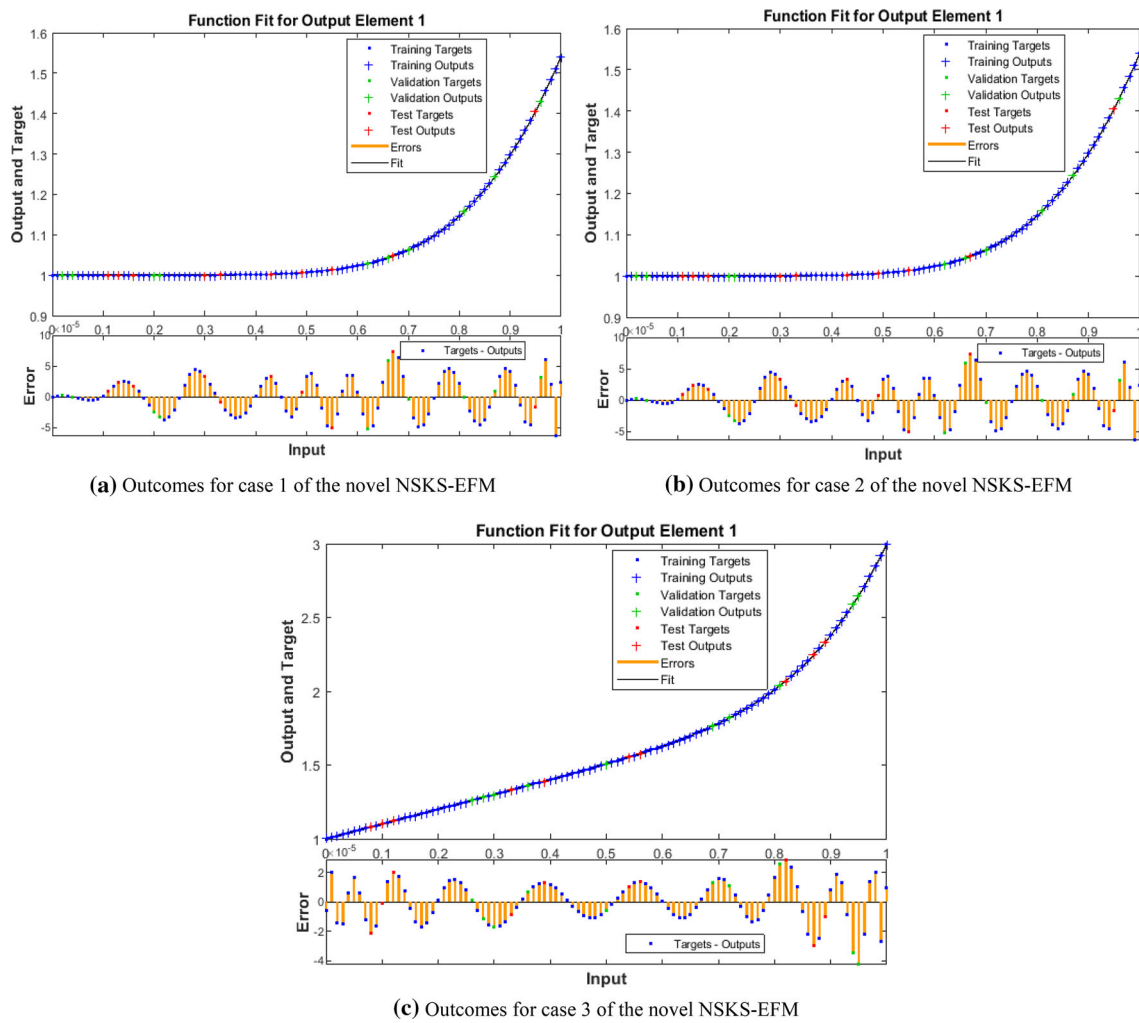


Fig. 6 Result comparison of the SNNs-LMBM with the reference dataset for different cases of the novel NSKS-EFM

Case 2: Consider the NSKS-EFM-based system using the multi-trigonometric ratios is written as:

$$\left\{ \begin{aligned} & \frac{d^7 \rho_1}{d\tau^7} + \frac{36}{\tau} \frac{d^6 \rho_1}{d\tau^6} + \frac{450}{\tau^2} \frac{d^5 \rho_1}{d\tau^5} + \frac{2400}{\tau^3} \frac{d^4 \rho_1}{d\tau^4} + \frac{4500}{\tau^4} \frac{d^3 \rho_1}{d\tau^3} \\ & + \frac{4320}{\tau^5} \frac{d^2 \rho_1}{d\tau^2} + \frac{720}{\tau^6} \frac{d\rho_1}{d\tau} + \rho_1 \rho_2 \\ & = 1 + 4656960 \cos(\tau) - 2174040\tau^2 \cos(\tau) \\ & + 48180\tau^4 \cos(\tau) - 85\tau^6 \cos(\tau) - \tau^{14} \cos^2(\tau) \\ & - 527200\tau \sin(\tau) + 442200\tau^3 \sin(\tau) \\ & - 2844\tau^5 \sin(\tau) + \tau^7 \sin(\tau), \\ & \frac{d^7 \rho_2}{d\tau^7} + \frac{36}{\tau} \frac{d^6 \rho_2}{d\tau^6} + \frac{450}{\tau^2} \frac{d^5 \rho_2}{d\tau^5} + \frac{2400}{\tau^3} \frac{d^4 \rho_2}{d\tau^4} + \frac{4500}{\tau^4} \frac{d^3 \rho_2}{d\tau^3} + \\ & \frac{4320}{\tau^5} \frac{d^2 \rho_2}{d\tau^2} + \frac{720}{\tau^6} \frac{d\rho_2}{d\tau} - \rho_1 \rho_2 \\ & = -1 - 4656960 \cos(\tau) + 2174040\tau^2 \cos(\tau) \\ & - 48180\tau^4 \cos(\tau) + 85\tau^6 \cos(\tau) + \tau^{14} \cos^2(\tau) \\ & + 527200\tau \sin(\tau) - 442200\tau^3 \sin(\tau) \\ & + 2844\tau^5 \sin(\tau) - \tau^7 \sin(\tau), \end{aligned} \right. \quad (36)$$

Case 3: Consider the NSKS-EFM based system using the singularity in its forcing function is written as:

$$\left\{ \begin{aligned} & \frac{d^7 \rho_1}{d\tau^7} + \frac{36}{\tau} \frac{d^6 \rho_1}{d\tau^6} + \frac{450}{\tau^2} \frac{d^5 \rho_1}{d\tau^5} + \frac{2400}{\tau^3} \frac{d^4 \rho_1}{d\tau^4} + \frac{4500}{\tau^4} \frac{d^3 \rho_1}{d\tau^3} \\ & + \frac{4320}{\tau^5} \frac{d^2 \rho_1}{d\tau^2} + \frac{720}{\tau^6} \frac{d\rho_1}{d\tau} + \rho_1^2 \rho_2 \\ & = 4656961 + \frac{720}{\tau^6} + 3\tau + 3\tau^2 + \tau^3 + \tau^7 + 2\tau^8 \\ & + \tau^9 - \tau^{14} - \tau^{15} - \tau^{21}, \\ & \frac{d^7 \rho_2}{d\tau^7} + \frac{36}{\tau} \frac{d^6 \rho_2}{d\tau^6} + \frac{450}{\tau^2} \frac{d^5 \rho_2}{d\tau^5} + \frac{2400}{\tau^3} \frac{d^4 \rho_2}{d\tau^4} + \frac{4500}{\tau^4} \frac{d^3 \rho_2}{d\tau^3} \\ & + \frac{4320}{\tau^5} \frac{d^2 \rho_2}{d\tau^2} + \frac{720}{\tau^6} \frac{d\rho_2}{d\tau} - \rho_1 \rho_2^2 \\ & = -4656961 + \frac{720}{\tau^6} - 3\tau - 3\tau^2 - \tau^3 + \tau^7 + 2\tau^8 \\ & + \tau^9 + \tau^{14} + \tau^{15} - \tau^{21}, \end{aligned} \right. \quad (37)$$

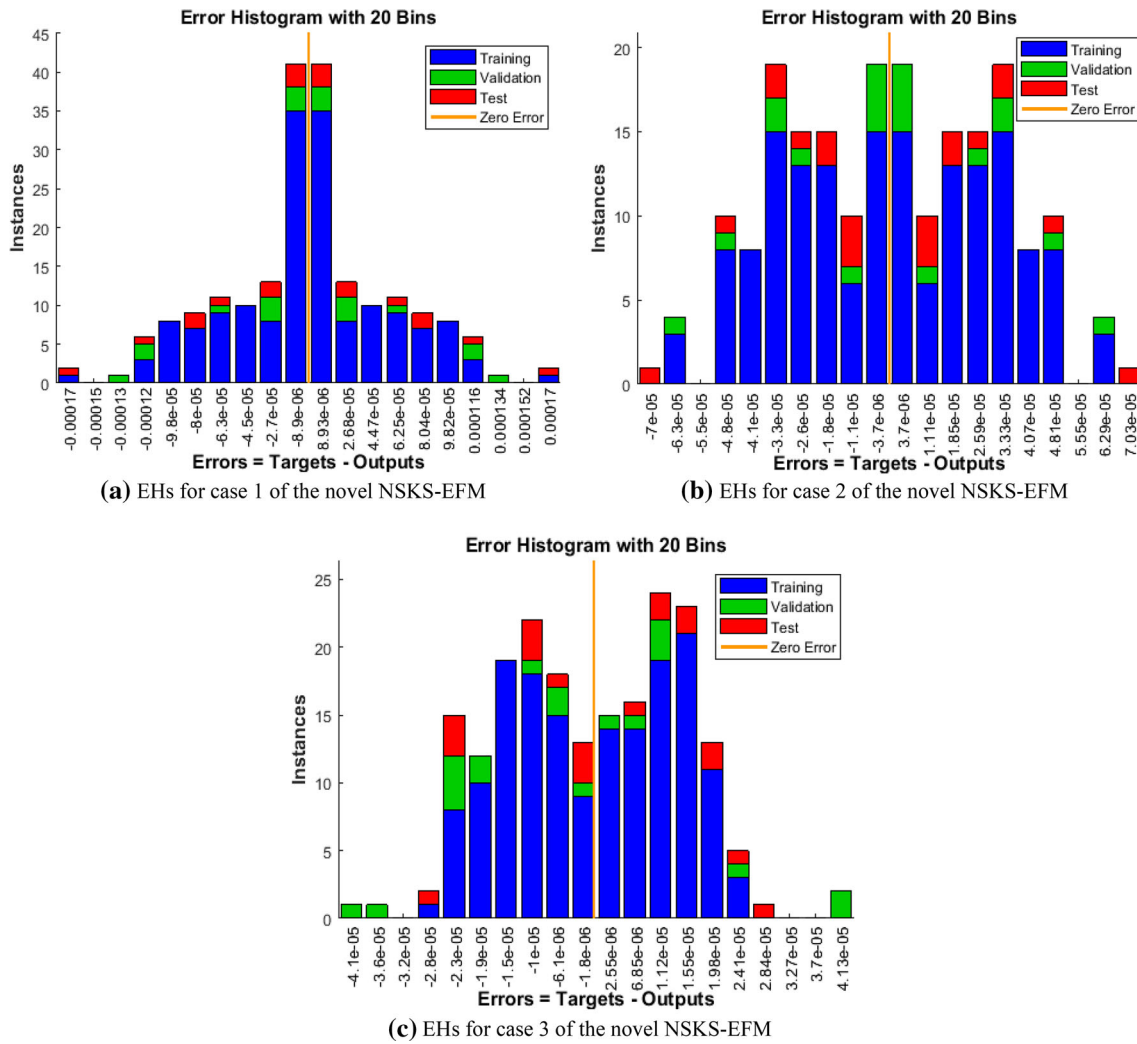


Fig. 7 EHs for the SNNs-LMBM to solve the NSKS-EFM based case 1

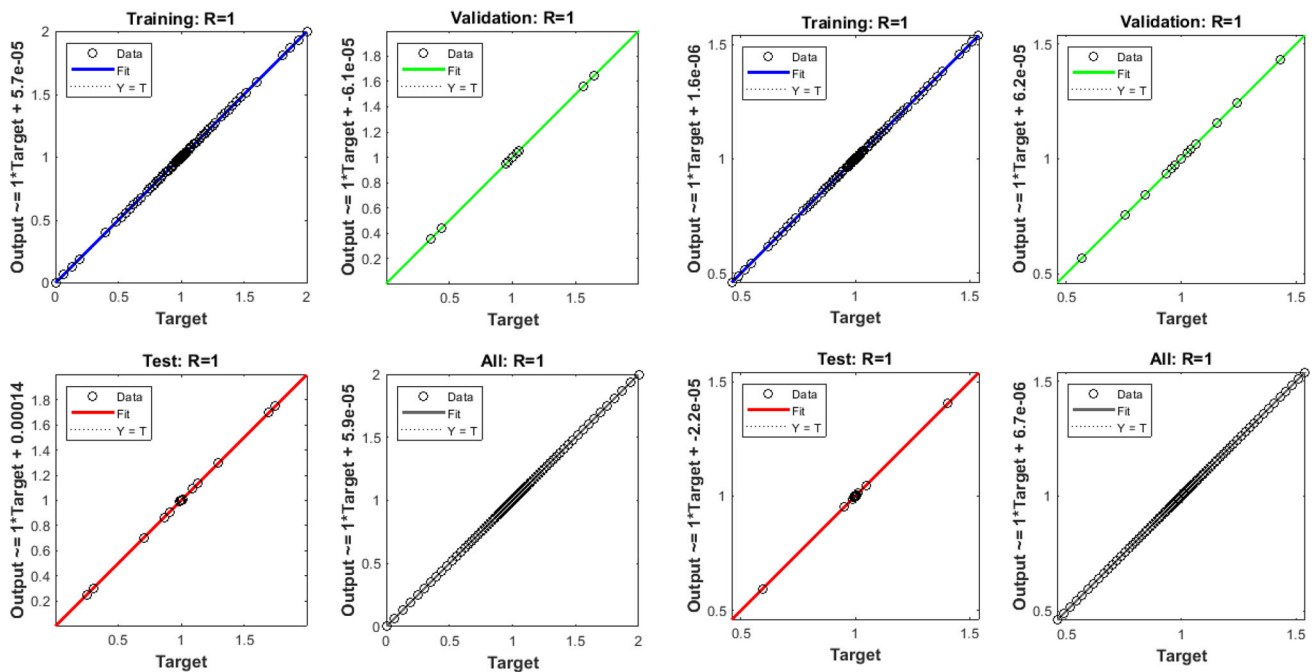
The ICs of the above systems (35-37) are provided as:

$$\begin{cases} \rho_1(0) = 1, \frac{d\rho_1(0)}{d\tau} = 0, \frac{d^2\rho_1(0)}{d\tau^2} = 0, \frac{d^3\rho_1(0)}{d\tau^3} = 0, \\ \frac{d^4\rho_1(0)}{d\tau^4} = 0, \frac{d^5\rho_1(0)}{d\tau^5} = 0, \frac{d^6\rho_1(0)}{d\tau^6} = 0 \\ \rho_2(0) = 1, \frac{d\rho_2(0)}{d\tau} = 0, \frac{d^2\rho_2(0)}{d\tau^2} = 0, \frac{d^3\rho_2(0)}{d\tau^3} = 0, \\ \frac{d^4\rho_2(0)}{d\tau^4} = 0, \frac{d^5\rho_2(0)}{d\tau^5} = 0, \frac{d^6\rho_2(0)}{d\tau^6} = 0. \end{cases} \quad (38)$$

The graphs of each case of the novel NSKS-EFM using the designed SNNs-LMBM are illustrated in Figs. 4–8. The graphical results of the novel NSKS-EFM based cases of type 1 based on the performance and transition states are provided in Figs. 4 and 5, respectively. The convergence through mean square error (MSE) using the testing, training, validation and best curve for each case of the novel NSKS-EFM is examined in Fig. 4. The performances of the best network are derived at epoch 55, 114 and 436 around 4.981×10^{-09} , 9.050×10^{-10} and 5.258×10^{-10} , respectively. The val-

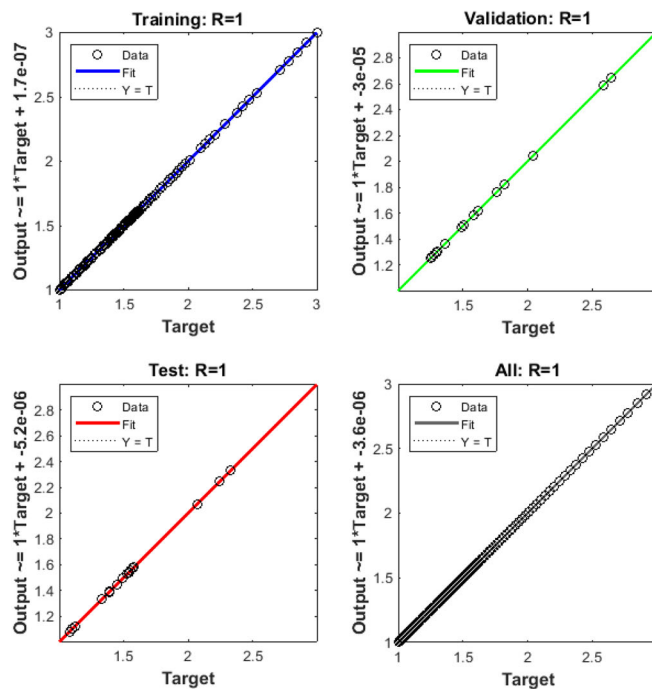
ues of the gradient using the step-size (μ) is estimated using the designed SNNs-LMBM for each case of novel NSKS-EFM are $[2.296 \times 10^{-06}, 9.050 \times 10^{-10}$ and $9.990 \times 10^{-08}]$ and $[1 \times 10^{-08}, 1 \times 10^{-09}$ and $1 \times 10^{-08}]$ illustrated in Fig. 5. These performances designate the convergence and correctness of the designed SNNs-LMBM for each case of novel NSKS-EFM.

Figure 6 illustrates the curve fitting values for each case of the novel NSKS-EFM. These plots specify the results comparison of the SNNs-LMBM with the reference dataset of the novel NSKS-EFM based type 1 along with the error plots. The maximum error values in the intervals of training, testing and validation for the designed SNNs-LMBM lie in the ranges of 10^{-05} to 10^{-07} for each case of the novel NSKS-EFM. The plots of EHs are illustrated in Fig. 7, which are performed to scrutinize the error investigations for the input and output grids to solve each case of the NSKS-EFM. The average values of EHs with zero-line reference found around 8.9×10^{-06} , 3.7×10^{-06} and 1.8×10^{-06} for cases 1, 2 and 3 of the novel NSKS-EFM.



(a) Outcomes for case 1 of the novel NSKS-EFM

(b) Outcomes for case 2 of the novel NSKS-EFM



(c) Outcomes for case 3 of the novel NSKS-EFM

Fig. 8 Regression plots for solving the different cases of the NSKS-EFM

The regression value plots are illustrated in Fig. 8 for each case of the NSKS-EFM. These graphical surveys using the co-relation values are derived to check the regression. It is noted that the correlation (R) values are found around 1 for each case of the NSKS-EFM, which designates the perfect model based on testing, validation and training. This mathematical behavior depicts

the precision of the SNNS-LMBM to solve the NSKS-EFM. Additionally, the convergence performance via MSE trials is achieved for the testing, training, performance, backpropagation actions, validation, performed epochs and time complexity are tabulated in Table 1 for solving the NSKS-EFM. One can see that the time consumed for the formulation of the networks by SNNS-

Table 1 SNNs-LMBM results for each case of the type-I of the novel NSKS-EFM

Case	Level of MSE for samples			Performance	Gradient	Mu	Epoch	Time
	Training value	Validation value	Testing value					
1	3.118×10^{-09}	4.981×10^{-09}	6.076×10^{-09}	2.43×10^{-09}	2.30×10^{-06}	1.00×10^{-08}	55	6
2	9.067×10^{-10}	9.050×10^{-10}	1.168×10^{-09}	9.07×10^{-10}	9.93×10^{-08}	1.00×10^{-09}	114	6
3	1.763×10^{-10}	5.258×10^{-10}	2.862×10^{-10}	1.76×10^{-10}	9.99×10^{-08}	1.00×10^{-08}	436	6

Fig. 9 Results comparison of the SNNs-LMBM for solving the NSKS-EFM

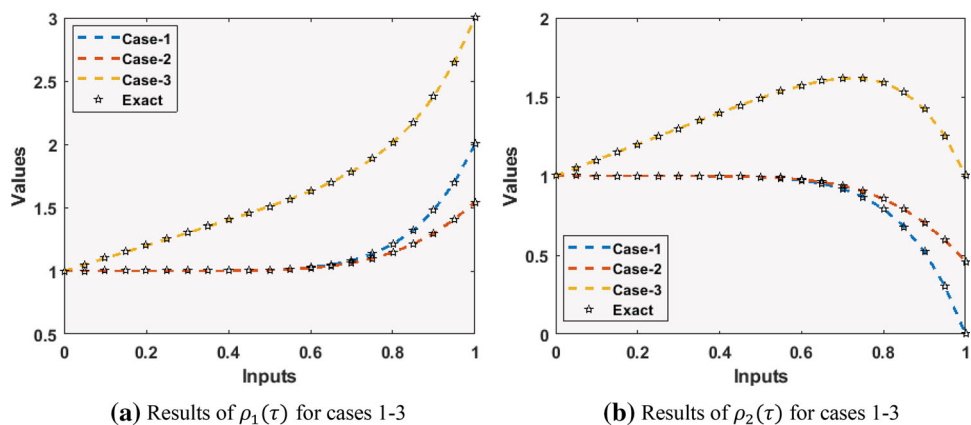
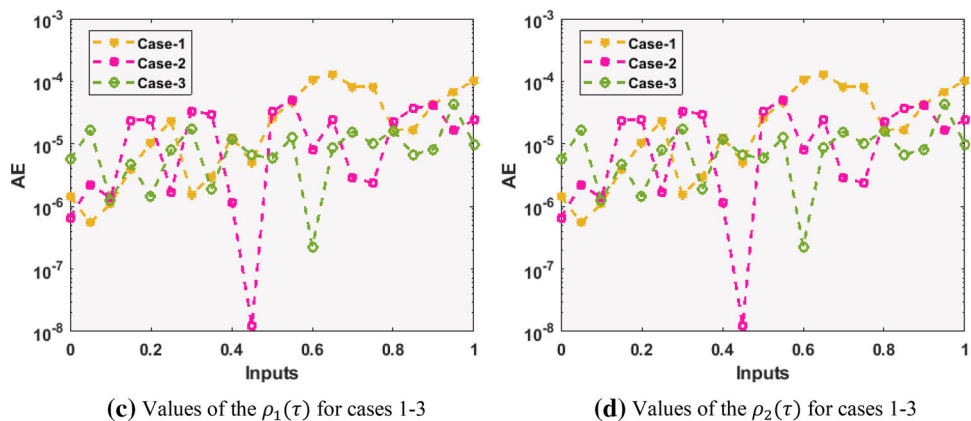


Fig. 10 AE values for the parameters $\rho_1(\tau)$ and $\rho_2(\tau)$ to solve the cases 1–3 using the novel NSKS-EFM



LMBM for 10 neurons is consistently around 6 second for all three cases of NSKS-EFM.

Figures 9 and 10 indicate the results comparison to solve the NSKS-EFM based cases 1–3. The results of the $\rho_1(\tau)$ and $\rho_2(\tau)$ using the novel NSKS-EFM based case 1 are illustrated in Fig. 9. It is observed that the results overlapping shows the accuracy and exactness of the designed SNNs-LMBM. The absolute error (AE) plots for each case of the NSKS-EFM are illustrated in Fig. 10. These AE values of the parameters $\rho_1(\tau)$ and $\rho_2(\tau)$ for cases 1-3 are drawn in Fig. 10. It is noticed that the values of the AE for the parameters $\rho_1(\tau)$ and $\rho_2(\tau)$ are found around $[10^{-05}, 10^{-08}]$ for each case. These overlapped values and good performances of the AE show the correctness of the novel model, as well as, reliable implementation of the designed SNNs-LMBM.

Conclusions

In this work, a novel nonlinear fractional seventh kind of singular Emden–Fowler model together with its six types is presented. This novel model is obtained with the use of the typical Emden–Fowler model. Three different cases of the first type of the novel model are presented using the comprehensive detail of the singularities and the shape factors. It is noticed that the multiple singularities as well as the shape factors are involved in the first five groups, whereas the last group has a single shape factor and singularity. The cases presented on the behalf of the first type of the novel model involve nonlinearity, multi trigonometric functions and singular terms in its forcing functions. To solve the designed singular seventh order model, a supervised neural network approach based on the Levenberg–Marquardt back-propagation is presented. The data for the approximation for training is 80% and both for validation and

testing is 10% using the optimal practice with 10 numbers of hidden neurons. To check the correctness of the designed system and proposed stochastic scheme, the overlapped plots have been obtained and the values of the AE are found in good measures. For the MSE, the convergence measures for the best curve, training, validation and testing are presented in each case of the novel model. The co-relation values are provided to show the regression and the gradient performances using the designed approach are assessed in each case of the novel model. Additionally, the accuracy and precision are justified by plotting the regression dynamics, EHs along with the convergence on MSE.

In future, the proposed scheme will be implemented to solve the system of equation represented in the fractional order problems, fluid mechanics models and mathematical models for information security [43–54].

Declarations

Conflict of interest The authors declare that they have no conflict of interest

References

1. Z. Shah et al., Design of neural network based intelligent computing for numerical treatment of unsteady 3D flow of Eyring-Powell magneto-nanofluidic model. *J. Market. Res.* **9**(6), 14372–14387 (2020)
2. M. Umar et al., A stochastic computational intelligent solver for numerical treatment of mosquito dispersal model in a heterogeneous environment. *Eur. Phys. J. Plus* **135**(7), 1–23 (2020)
3. I. Jadoon et al., Integrated meta-heuristics finite difference method for the dynamics of nonlinear unipolar electrohydrodynamic pump flow model. *Appl. Soft Comput.* **97**, 106791 (2020)
4. I. Jadoon et al., Design of evolutionary optimized finite difference based numerical computing for dust density model of nonlinear Van-der Pol Mathieu's oscillatory systems. *Math. Comput. Simul.* **181**, 444–470 (2021)
5. A.H. Bukhari et al., Design of a hybrid NAR-RBFs neural network for nonlinear dusty plasma system. *Alex. Eng. J.* **59**(5), 3325–3345 (2020)
6. M. Umar et al., Stochastic numerical technique for solving HIV infection model of CD4+ T cells. *Eur. Phys. J. Plus* **135**(6), 403 (2020)
7. K. Boubaker et al., Application of the BPES to Lane-Emden equations governing polytropic and isothermal gas spheres. *New Astron.* **17**(6), 565–569 (2012)
8. J.S. Wong, On the generalized Emden-Fowler equation. *SIAM Rev.* **17**(2), 339–360 (1975)
9. A.M. Wazwaz, Adomian decomposition method for a reliable treatment of the Emden-Fowler equation. *Appl. Math. Comput.* **161**(2), 543–560 (2005)
10. A. Taghavi et al., A solution to the Lane-Emden equation in the theory of stellar structure utilizing the Tau method. *Math. Methods Appl. Sci.* **36**(10), 1240–1247 (2013)
11. Z. Sabir et al., Novel design of Morlet wavelet neural network for solving second order Lane-Emden equation. *Math. Comput. Simul.* **172**, 1–14 (2020)
12. W. Adel et al., Solving a new design of nonlinear second-order Lane-Emden pantograph delay differential model via Bernoulli collocation method. *Eur Phys J Plus* **135**(6), 427 (2020)
13. K. Nisar et al., Evolutionary Integrated Heuristic with Gudermannian Neural Networks for Second Kind of Lane-Emden Nonlinear Singular Models. *Appl. Sci.* **11**(11), 4725 (2021)
14. R. Singh et al., Haar wavelet collocation approach for Lane-Emden equations arising in mathematical physics and astrophysics. *Eur. Phys. J. Plus* **134**(11), 548 (2019)
15. F. Abbas et al., Approximate solutions to lane-emden equation for stellar configuration. *Appl. Math. Inf. Sci.* **13**, 143–152 (2019)
16. S. Chandrasekhar, *An Introduction to the Study of Stellar Structure* (Dover Publications, New York, 1967)
17. T. Luo et al., Nonlinear asymptotic stability of the Lane-Emden solutions for the viscous gaseous star problem with degenerate density dependent viscosities. *Commun. Math. Phys.* **347**(3), 657–702 (2016)
18. A.H. Bhrawy et al. An efficient collocation method for a class of boundary value problems arising in mathematical physics and geometry. in *Abstract and Applied Analysis*, vol. 2014. (Hindawi Publishing Corporation, 2014)
19. J.A. Khan et al., Nature-inspired computing approach for solving non-linear singular Emden-Fowler problem arising in electromagnetic theory. *Connect. Sci.* **27**(4), 377–396 (2015)
20. J. Džurina, S.R. Grace, I. Jadlovská, T. Li, Oscillation criteria for second-order Emden-Fowler delay differential equations with a sublinear neutral term. *Math. Nachr.* **293**, 1–13 (2020). <https://doi.org/10.1002/mana.201800196>
21. M. Dehghan et al., Solution of an integro-differential equation arising in oscillating magnetic fields using He's homotopy perturbation method. *Progr. Electromagnet. Res.* **78**, 361–376 (2008)
22. J.I. Ramos, Linearization methods in classical and quantum mechanics. *Comput. Phys. Commun.* **153**(2), 199–208 (2003)
23. V. Radulescu et al., Combined effects in nonlinear problems arising in the study of anisotropic continuous media. *Nonlinear Anal. Theory Methods Appl.* **75**(3), 1524–1530 (2012)
24. Z. Sabir et al., A neuro-swarming intelligence-based computing for second order singular periodic non-linear boundary value problems. *Front. Phys.* **8**, 224 (2020)
25. Z. Sabir et al., Design of stochastic numerical solver for the solution of singular three-point second-order boundary value problems. *Neural Comput. Appl.* **33**(7), 2427–2443 (2021)
26. Z. Sabir et al. Integrated intelligence of neuro-evolution with sequential quadratic programming for second-order Lane-Emden pantograph models. in *Mathematics and Computers in Simulation* (2021)
27. Z. Sabir et al., Solution of novel multi-fractional multi-singular Lane-Emden model using the designed FMNE-ICS. *Neural Comput. Appl.* **33**(24), 17287–17302 (2021)
28. M.A. Abdelkawy et al., Numerical investigations of a new singular second-order nonlinear coupled functional Lane-Emden model. *Open Phys.* **18**(1), 770–778 (2020)

29. K. Parand et al., Rational Legendre approximation for solving some physical problems on semi-infinite intervals. *Phys. Scr.* **69**(5), 353 (2004)
30. Z. Sabir et al., Neuro-evolution computing for nonlinear multi-singular system of third order Emden-Fowler equation. *Math. Comput. Simul.* **185**, 799–812 (2021)
31. J.L. Guirao et al. Design and numerical solutions of a novel third-order nonlinear Emden–Fowler delay differential model. In: *Mathematical Problems in Engineering* (2020)
32. Z. Sabir et al., Design of neuro-swarmling-based heuristics to solve the third-order nonlinear multi-singular Emden-Fowler equation. *Eur. Phys. J. Plus* **135**(6), 1–17 (2020)
33. N.T. Shawagfeh, Non-perturbative approximate solution for Lane-Emden equation. *J. Math. Phys.* **34**(9), 4364–4369 (1993)
34. J.I. Ramos, Series approach to the Lane-Emden equation and comparison with the homotopy perturbation method. *Chaos Solitons Fract.* **38**(2), 400–408 (2008)
35. A.K. Dizicheh, S. Salahshour, A. Ahmadian, D. Baleanu, A novel algorithm based on the Legendre wavelets spectral technique for solving the Lane–Emden equations. in *Applied Numerical Mathematics* (2020)
36. U. Saeed, Haar Adomian method for the solution of fractional nonlinear Lane-Emden type equations arising in astrophysics. *Taiwan. J. Math.* **21**(5), 1175–1192 (2017)
37. M.S. Hashemi et al., Solving the Lane-Emden equation within a reproducing kernel method and group preserving scheme. *Mathematics* **5**(4), 77 (2017)
38. Z. Sabir et al. On a new model based on third-order nonlinear multi singular functional differential equations. in *Mathematical Problems in Engineering* (2020)
39. Z. Sabir et al., Heuristic computing technique for numerical solutions of nonlinear fourth order Emden-Fowler equation. *Math. Comput. Simul.* **178**, 534–548 (2020)
40. Z. Sabir et al., FMNEICS: fractional Meyer neuro-evolution-based intelligent computing solver for doubly singular multi-fractional order Lane-Emden system. *Comp. Appl. Math.* **39**, 303 (2020). <https://doi.org/10.1007/s40314-020-01350-0>
41. Z. Sabir et al., Integrated intelligent computing paradigm for nonlinear multi-singular third-order Emden-Fowler equation. *Neural Comput. Appl.* **33**(8), 3417–3436 (2021)
42. Z. Sabir et al., Meyer wavelet neural networks to solve a novel design of fractional order pantograph Lane-Emden differential model. *Chaos Solitons Fract.* **152**, 111404 (2021)
43. H. Günerhan, E. Çelik, Analytical and approximate solutions of fractional partial differential-algebraic equations. *Appl. Math. Nonlinear Sci.* **5**(1), 109–120 (2020)
44. H.M. Baskonus et al., New complex hyperbolic structures to the lonngren-wave equation by using sine-gordon expansion method. *Appl. Math. Nonlinear Sci.* **4**(1), 141–150 (2019)
45. A. Yokuş, S. Gülbahar, Numerical solutions with linearization techniques of the fractional Harry Dym equation. *Appl. Math. Nonlinear Sci.* **4**(1), 35–42 (2019)
46. J. Wu, J. Yuan, W. Gao, Analysis of fractional factor system for data transmission in SDN. *Appl. Math. Nonlinear Sci.* **4**(1), 191–196 (2019)
47. H. Duru et al., New analytical solutions of conformable time fractional bad and good modified Boussinesq equations. *Appl. Math. Nonlinear Sci.* **5**(1), 447–454 (2020)
48. D.W. Brzeziński, Review of numerical methods for NumILPT with computational accuracy assessment for fractional calculus. *Appl. Math. Nonlinear Sci.* **3**(2), 487–502 (2018)
49. E. İlhan, I.O. Kıymaz, A generalization of truncated M-fractional derivative and applications to fractional differential equations. *Appl. Math. Nonlinear Sci.* **5**(1), 171–188 (2020)
50. S.E. Awan et al., Numerical treatments to analyze the nonlinear radiative heat transfer in MHD nanofluid flow with solar energy. *Arab. J. Sci. Eng.* **45**(6), 4975–4994 (2020)
51. T. Sajid, et al. Impact of activation energy and temperature-dependent heat source/sink on maxwell-sutterby fluid. in *Mathematical Problems in Engineering* (2020)
52. M. Modanli, A. Akgül, On Solutions of Fractional order Telegraph partial differential equation by Crank-Nicholson finite difference method. *Appl. Math. Nonlinear Sci.* **5**(1), 163–170 (2020)
53. T. Sajid et al., Upshot of radiative rotating Prandtl fluid flow over a slippery surface embedded with variable species diffusivity and multiple convective boundary conditions. *Heat Transf.* **50**(3), 2874–2894 (2021)
54. T. Sajid et al., Impact of oxytactic microorganisms and variable species diffusivity on blood-gold Reiner-Philippoff nanofluid. *Appl. Nanosci.* **11**(1), 321–333 (2021)